Nature of Exciton−Exciton Annihilation in an Aggregated Cyanine Dye

Serdar Özçelik and Daniel L. Akins*

Center for Analysis of Structures and Interfaces (CASI), Department of Chemistry, The City College of The City University of New York, New York, New York 10031

Received: February 5, 1997[⊗]

For aggregated 1,1′,3,3′-tetraethyl-5,5′,6,6′-tetrachlorobenzimidazolocarbocyanine (TTBC) adsorbed onto silica, we have ascertained that coherent optical dynamical processes play key roles in defining the temporal response and spectral profile of the fluorescence. We have also determined which coherent processes are involved in what might generally be termed exciton−exciton annihilation. Additionally, we provide in the TTBC system a concrete example of room temperature superradiance.

I. Introduction

Exciton−exciton annihilation is phenomenologically defined as a Stern−Volmer type quenching of emission from an excitonic state, which accompanies an increase in concentration of excited species (i.e., the emission intensity approaches a limiting value). Other phenomenological indicators of the presence of exciton−exciton annihilation are excitation intensity induced diminution of the emission lifetime and quantum yield, hypsochromic shifting of the peak frequency of the emission, and narrowing of the spectral profile of the emission.

The purpose of this report is to provide new insight into the phenomenon of exciton−exciton annihilation as derived from a study of an aggregated cyanine dye. Specifically, we have observed all such above mentioned phenomenological expressions of exciton−exciton annihilation in a system composed of 1,1′,3,3′-tetraethyl-5,5′,6,6′-tetrachlorobenzimidazolocarbocyanine (referred to hereinafter as TTBC; see Figure 1, bottom, for structure) adsorbed onto silica, in which TTBC exists in an aggregated state.[1] In this Letter, we focus on mechanistic details of exciton−exciton annihilation in aggregated TTBC, deciphered from time-resolved emission spectra of various excitonic states, to shed light on specific optical dynamical steps in the exciton−exciton annihilation process.

We report our finding for the TTBC system that coherent optical dynamical processes dictate the temporal and frequency content of the emitted radiation, and we identify the coherent processes involved in what is generally termed exciton−exciton annihilation. Furthermore, we provide in the TTBC system a concrete example of room temperature superradiance.

II. Experimental Section

All spectroscopic measurements were conducted at room temperature. TTBC was purchased from Accurate Chemical and Scientific Co., Westbury, NY, and used without further purification. The colloidal silica suspension was purchased from Aldrich Chemical Co., Milwaukee, WI. Specifications supplied for the silica colloid indicate 40% by weight in water of silica, pH = 9.7, specific surface area of 220 m^2/g, average diameter of 12 nm, average surface area of 452 nm^2, and viscosity of 16 cP.

Absorption spectra were recorded using a Perkin-Elmer Lambda 19, UV−vis/near-IR spectrometer. Steady-state fluorescence spectra were acquired using a SPEX Fluorolog-τ2 spectrofluorometer. Time-dependent emission measurements utilized a Hamamatsu streak camera, Model C4334, optically coupled to a charge-coupled-device (CCD) array detector. This system allowed the measurements of both the emission decay rate and the time-resolved emission spectrum. For this latter study a Chromex 250i imaging spectrometer was used. The ultimate time resolution that we have been able to attain with this system, using Hamamatsu U4290 fluorescence analysis software, is estimated to be better than 10 ps.

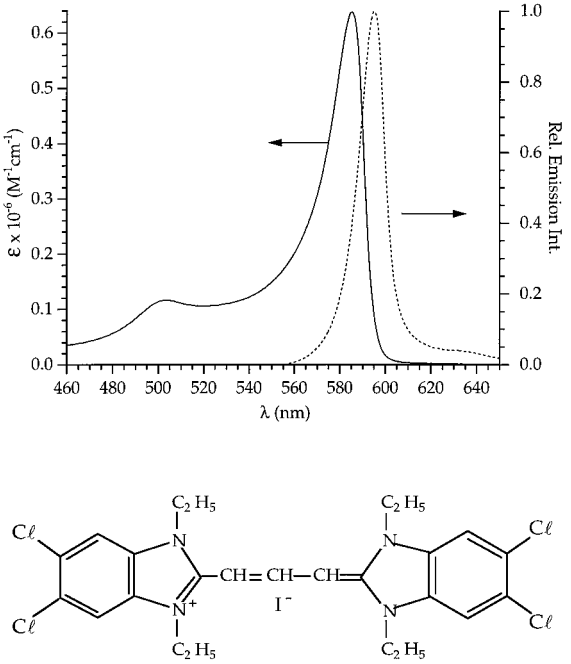

Figure 1. Absorption and emission spectra of adsorbed, J-aggregated TTBC. Chemical structure below spectra is that of TTBC.

The exciting light source for the emission studies was a Coherent 702 mode-locked, picosecond dye laser that was pumped by a Coherent Antares 76s Nd:YAG laser. The excitation wavelength, which overlaps the J-aggregate absorption (see Figure 1), was ca. 570 nm. For the present study, a high-pass filter (transmitting for wavelengths greater than 580 nm) was placed at the entrance slit of the Chromex spectrometer.

In order to prepare J-aggregated TTBC, 5 mL of 1.2 mM TTBC in methanol was mixed with 42 mL of silica colloid. The samples were excited with pulses of energy of ca. 0.26 nJ/pulse and 10 ps of duration, with a repetition rate of 76 MHz. The intensity of the incident radiation was adjusted through the use of calibrated neutral density filters to minimize lifetime-shortening effects associated with "high" excitation intensity,[2]

[⊗] Abstract published in *Advance ACS Abstracts,* April 1, 1997.

S1089-5647(97)00429-X CCC: $14.00

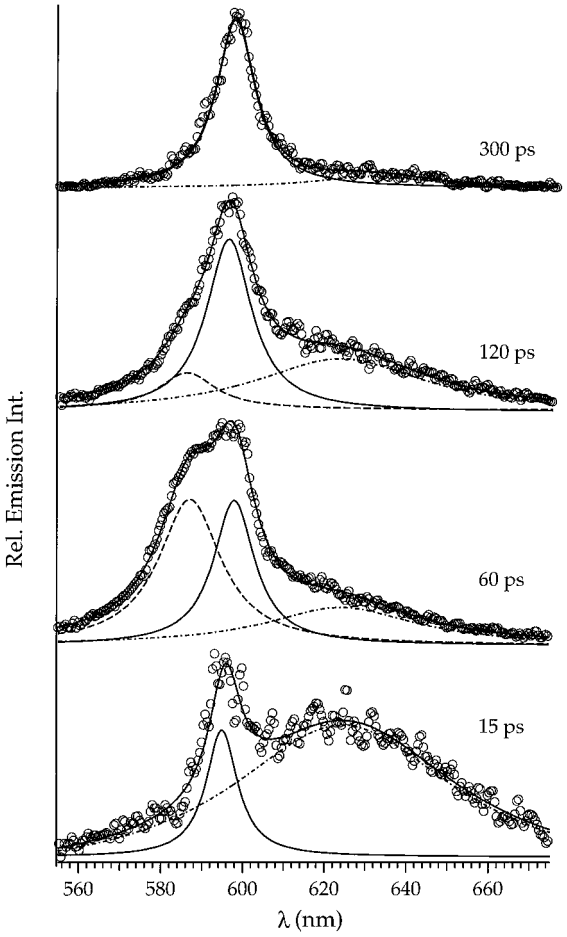

Figure 2. Representative time-resolved emission spectra of TTBC. A 25 ps time window was used. Decomposed spectra are shown for the one-exciton (solid line spectra that does not pass directly through data points), two-exciton (dashed line spectra), and red-emitter spectra (dash−dot spectra). Excitation wavelength was ca. 570 nm. The solid line spectra passing through data represent the sum of the spectra due to the one-, two-, and red-emitter components.

and front-surface luminescence measurements, using an optical waveguide to collect emission, were conducted (generally) on a static system, as opposed to a flowing system.

Data analysis and plotting of spectra utilized IGOR from Wavematrics (Lake Oswego, OR). This software also allowed decomposition of measured time-resolved spectral profiles in terms of a broad range of functional forms, such as Gaussians, Lorentzians, etc. For our present results, Lorentzian decompositions proved excellent.

III. Results and Discussion

Figure 1 shows absorption and emission spectra of J-aggregated TTBC. The absorption spectrum has two prominent bands, one at 500 nm and the other at 585 nm. The band at 585 nm is attributable to the 0−0 vibronic band, while that at 500 nm has been shown by excitation spectra of the fluorescence, which closely mimics the absorption spectrum, to correspond to a transition from the ground state to a higher vibronic state of the J-aggregate.[3] The emission spectrum consists of one band at 595 nm with a weak shoulder at ca. 630 nm.

Figure 2 shows representative time-resolved emission spectra of J-aggregates of TTBC following excitation with the 10 ps laser pulses. The time-resolved emission spectra can be analyzed to provide information concerning which emission components, as represented, for example, by their peak emission

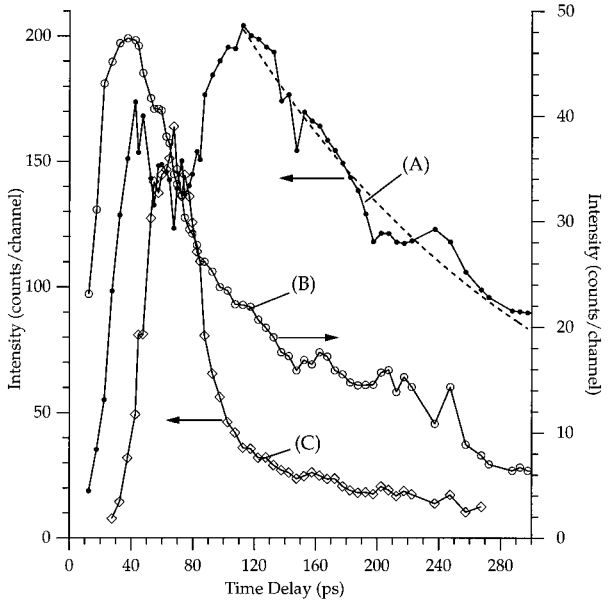

Figure 3. Time-resolved peak intensities for the one-exciton (A), red-emitter (B), and two-exciton (C) species extracted from data such as provided in Figure 2. The dashed line curve that overlaps data for the one-exciton peak emissions is a least-squares fit to the asymptotic form for $I(t)$.

wavelengths, contribute to the emission decay and, from such measurements, their intensity/time profiles. To this end, time-resolved spectra were decomposed in terms of Lorentzian functional forms. As indicated in Figure 2, the fluorescence spectrum can be decomposed into as many as three emission components, depending on the time delay. The time-resolved peak intensities of the three components, for an incident pulse energy of ca. 0.26 nJ/pulse, are provided in Figure 3.

Analysis of Figure 3 suggests that the 600 nm (curve A) emitter, i.e., the one-exciton species by analogy with designations specified by van Burgel *et al.*,[3] is formed early in the excitation process. Also, an emission feature at 625 nm (a red emitter; curve B) forms near $t = 0$, within the excitation pulse width, reaches a maximum around 50 ps following the laser pulse, and decays slowly thereafter.

A blue emitter (curve C), with wavelength maximum at 585 nm, also is evidenced in the decomposed, time-resolved profiles of Figure 2 (see also ref 4). This blue emitter makes is first discernible (due to the temporal resolution inherent in the spectral decomposition algorithm) ca. 20 ps after the initial excitation. It attains maximum intensity at ca. 80 ps and rapidly decays. After ca. 250 ps, the blue emission is essentially exhausted.

The observations for the time-resolved peak intensities of the various emitting species are consistent with the presence of one-exciton, two-exciton, and a long-lived, red-emitting species, the former two described by van Burgel *et al.*[4] The red-emitting species was originally assumed by us to be an aggregate of shorter coherence length than that associated with the one-exciton, since this concept has been advanced in earlier studies.[5,6] However, continuing studies suggest that this emission emanates from reabsorption of one-exciton emission. Specific measurements that have been performed that do not result in a red-emitting component include use of fluorescence cells of thickness 1 mm as opposed to the 1 cm cells in the studies that result in the data shown in Figure 2 and lower concentrations of TTBC.[1]

The temporally resolved emission spectra for the one- and two-exciton species have been analyzed by us in terms of a

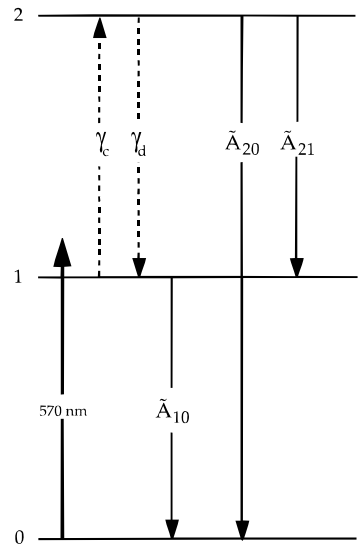

Figure 4. Photodynamic scheme to explain time-resolved dynamics of emitting species in the TTBC system. Levels 1 and 2 are shown as single levels for presentation purposes but represent bands of *k*-states, as is usual for composite states defined through molecular exciton theory. The tilde above the rate constants indicates that nonradiative processes can also participate in populating the final state of the transition.

population kinetics scheme,[1] which is similar to that applied by van Burgel *et al*.[4] Our scheme differs in the nature of the excitation process and the incorporation of a stimulated emission elementary kinetic step that couples emission from the one-exciton and two-exciton states.[1]

The energy level structure and population dynamics scheme that we employ is shown in Figure 4. Incident excitation is viewed as fully populating the one-exciton state, which is represented by a single energy level (specifically, the $k = 1$ emitting level of the linear aggregate), though, in reality, it is a band of states. It is implicit in Figure 4 that excitation is to higher one-exciton *k*-states in the exciton manifold that must relax to the emitting level; this relaxation, for our model, leads to the delay and finite rise time, following absorption of the incident photons, before attainment of peak-emission intensities by the emitting species. Subsequent steps in the population dynamics scheme relate to formation of a two-exciton species (defined as an aggregate containing two single-molecule excitations within its coherence length) and various emissions between states. For our system, we do not envisage creation of a two-exciton state through absorption of a second photon by a one-exciton aggregate (because of the low incident intensities). Rather, diffusional contact between one-exciton entities and dissociation of and emission from such entities help determine overall population dynamics.

In Figure 4, the numerals 0, 1, and 2 relate to ground, one-exciton, and two-exciton states, respectively. The Arabic numeral subscripts specify the energy states between which a transition can occur. For example, $\tilde{A}_{21}$ is the transition probability for conversion of the two-exciton state into the one-exciton state; the transition implicitly involves both radiative and nonradiative pathways. For all other subscripts, as for $\tilde{A}_{21}$, the first Arabic numeral identifies the upper state in the transition process. The Greek symbols with Latin subscripts, e.g., γ_c and γ_d, as defined by van Burgel *et al*.,[4] are the rate constants, respectively, for forming a two-exciton entity through collision (as a result of diffusion) between two one-exciton entities and the spontaneous dissociation of a two-exciton entity to give two one-exciton entities.

The simplified scheme shown in Figure 4 leads to a system of rate equations relating the populations of the various states to one another. The resultant populations must be multiplied by appropriate emission probabilities before they can be related to the time-dependent, spectrally resolved peak intensities of Figure 3. It is also to be noted that only the one-exciton state is pumped, and, furthermore, our equations address the decay dynamics for the one-exciton state as population is created by a relaxation from higher *k*-states of the one-exciton manifold, through the formation factor $F(t)$. Additionally, for the two-exciton state, the dynamics over the full experiment time frame is implicit in the scheme, since aggregates that have the two-exciton state populated are viewed as derived through "collisions" between extant, mobile one-excitons.

The rate equations appropriate for the elementary excited state dynamics indicated in Figure 4 are provided below. (Which terms appear in the equations and why are discussed following the equations.)

$$\frac{dn_1}{dt} = F(t) - \tilde{A}_{10}n_1 - \gamma_c n_1^2 + (\tilde{A}_{21} + 2\gamma_d)n_2 - B_{12}(n_2\, e^{-A_{21}t})n_1 \quad (1)$$

$$\frac{dn_2}{dt} = \frac{\gamma_c}{2}n_1^2 - (\tilde{A}_{21} + \tilde{A}_{20} + \gamma_d)n_2 - B_{10}(n_1\, e^{-A_{10}t})n_2 \quad (2)$$

In these equations, transition probabilities such as $\tilde{A}_{10}$ correspond to rates of change of population that incorporate both radiative and nonradiative pathways. As a result $\tilde{A}_{ij} = A_{ij}/\phi_{ij}$, where ϕ_{ij} is the quantum yield for radiative decay and A_{ij} is the spontaneous emission rate constant.

Other important factors in eqs 1 and 2 are those containing the term B_{ij}, the transition probability for induced absorption or emission (note, $B_{ij} = B_{ji}$ and $A_{21} = (8\pi\nu_{21}^2/c^3)B_{12}$, with c being the speed of light), the term involving $n_2\, e^{-A_{21}t}$, which corresponds to the radiative density, and the product $n_i n_j$ that causes the nonlinear differential equations for n_1 to assume a competition/cooperation character and to fall into the class of functions termed Volterra equations.[7,8]

A rationalization for the presence of the term involving radiation-induced transition rates in the coupled equations is obviously required. This rationalization derives from interpreting the time dependence of the intensities of emission from the one-exciton and two-exciton states shown in Figure 3. What is immediately clear is that growth of the two-exciton emission is at the expense of the one-exciton emission. In fact, a so-called "predator−prey" relationship, common for Volterra equations, appears to exist, where a maximizing of the predator's population results in a minimizing of the prey's population. This "coupling" between the two populations for our system is deduced as being due to stimulated emission of one-exciton photons, in the spectral region that overlaps photons arising from transitions between the two-exciton state and the one-exciton state. In other words, the intensity of the two-exciton emission at ν_{21} is augmented (amplified) by induced emission of one-exciton state emitters, but at the frequency ν_{21}, instead of ν_{10}, which is possible because of the overlapping emission profiles. Such an eventuality seems all the more reasonable since a resultant one-exciton aggregate (on the same domain that defines the aggregate) is per force exposed to the emitted radiation field when a two-exciton is emitted. Reciprocity where ν_{10} photons would be expected to induce a decrease in the population of the n_2 state would seem not to be mandated, since there exists no two-exciton entity on the same aggregate that can be induced to emit. Thus a stimulated emission term coupling n_1 and n_2 might not be important in eq 2. However, we should note that a more long-range, interdomain optical coupling could be

applicable and would require incorporation of effects of ν_{10} and ν_{21} photons in stimulated emission terms in eqs 1 and 2.

Now we address the solutions of the two coupled Volterra equations. No general analytical solutions are known by the authors to exist; however, approximate solutions are discussed elsewhere.[9]

Determination of the parameters in eq 1, for the asymptotic situation where n_2 has passed its peak intensity and has decreased, was made; the fact that the coefficient for radiative transition between the two-exciton and ground states is forbidden in the dipolar approximation, since it requires the simultaneous transition of two electrons, was also utilized.[1] For this case, with $t > t_l$, a time (t_l) after which the population of n_2 has a small value and yet n_1 is still substantial, the differential equation for n_1, with the rate of formation term having gone to zero also, assumes the form

$$\frac{dn_1}{dt} + \tilde{A}_{10} n_1 + \gamma_c n_1^2 = 0 \tag{3}$$

a Ricatti's equation,[7] which can be exactly solved to give the relation

$$n_1(t \geq t_l) = \frac{n_1^\circ \tilde{A}_{10}\, e^{-\tilde{A}_{10} t}}{(\gamma_c n_1^\circ + \tilde{A}_{10}) - \gamma_c n_1^\circ\, e^{-\tilde{A}_{10} t}} \tag{4}$$

where $n_1^\circ = n_1(t = t_l)$. Equation 3 is essentially the same one as solved by van Burgel *et al.*,[4] although the solution reported by them is not equivalent to eq 4.

For $t_l \approx 100$ ps, the emission rate constants returned by a least-squares fit to the n_1 data in Figure 4 are $\tilde{A}_{10} = 1.13 \times 10^{-3}$ ps^{-1} and $K \times \phi_{10}/\gamma_c = 3.4 \times 10^{+7}$ ps, where K is the proportionality constant that accounts for the instrument response and signal collection geometry factors. The first of these values indicates a fluorescence lifetime of 889 ps for the one-exciton state.

The value for the lifetime of the one-exciton to ground transition (τ_{10}) is about a factor of $^1/_3$ of the monomeric TTBC room temperature lifetime, as measured in this laboratory,[2] and can be classified as indicating superradiance, assuming the radiation quantum yield is close to 1. We might note that even should ϕ_{10} differ substantially from 1, the system may still be considered superradiant because of the effect of temperature on emission rates: for example, it has been shown that emission is generally allowed from a low k-state of the aggregate, while higher temperatures lead to population of nonradiating k-states and an increased lifetime as energy within the aggregate must relax below a threshold level defined by the emitting state.[10]

IV. Conclusions

Our findings indicate that what might pass as exciton−exciton annihilation in aggregated TTBC is, in fact, induced emission from a one-exciton state caused by two-exciton photons. The sequence of events indicated is that two one-excitons come together and create a two-exciton species. This species, upon emission, induces or stimulates another one-exciton species to give up a photon and return to the ground state. The net results of these photodynamical steps are that two one-excitons come together in the beginning and a single one-exciton remains in the end. During this process coherent, amplified emission of a photon from the two-exciton state occurs.

We infer that similar (if not identical) optical dynamical steps apply for other systems as well, where exciton−exciton annihilation has been invoked as a catch all phenomenological term to describe coherent effects that evolve with increase in exciton density, including possibly even photosynthetic antenna systems.

Lastly, we note that the TTBC aggregate system exhibits superradiance, and this process is intimately connected to the existence of stimulated emission at the two-exciton to one-exciton emission frequency.

Acknowledgment. Support for this research by the National Science Foundation (NSF) under Grant HRD-9353488 and by NASA under its FAR program is gratefully acknowledged.

References and Notes

(1) Özçelik, S.; Akins, D. L. Dynamics of Interacting Excitons in an Adsorbed J-Aggregated Cyanine Dye. To be submitted for publication in *J. Phys. Chem.*

(2) Sundström, V.; Gillbro, T.; Gadonas, R. A.; Piskarskas, A. *J. Chem. Phys.* **1988**, *89*, 2754.

(3) Özçelik, Serdar. Spectroscopic and Dynamic Properties of Molecules Adsorbed on Surfaces. Ph.D. Dissertation, The City University of New York, 1996; p 126.

(4) van Burgel, M.; Wiersma, D. A.; Duppen, K. *J. Chem. Phys.* **1995**, *102*, 20.

(5) Manabe, Y.; Tokihiro, T.; Hanamura, E. *Phys. Rev. B.* **1993**, *48*, 2773.

(6) Akins, D. L.; Özçelik, S.; Zhu, H.-R.; Guo, C. *J. Phys. Chem.* **1996**, *100*, 14390.

(7) Goel, N. S.; Maitra, S. C.; Montroll, E. W. *On the Volterra and Other Nonlinear Models of Interacting Populations*; Academic Press: New York, 1971.

(8) Davis, H. T. *Introduction to Nonlinear Differential and Integral Equations*; Dover Publications: New York, 1962.

(9) Akins, D. L. Optical Dynamics of Interacting One- and Two-Excitons: Equations and Solutions. To be submitted for publication in *J. Phys. Chem.*

(10) Kamalov, V. F.; Struganova, I. A.; Tani, T.; Yoshihara, K. *Chem. Phys. Lett.* **1994**, *220*, 257.